# UC San Diego
## UC San Diego Previously Published Works

**Title**
Hyaluronan Breakdown Contributes to Immune Defense against Group A Streptococcus *

**Permalink**
https://escholarship.org/uc/item/5qf584hn

**Journal**
Journal of Biological Chemistry, 289(39)

**ISSN**
0021-9258

**Authors**
Schommer, Nina N
Muto, Jun
Nizet, Victor
et al.

**Publication Date**
2014-09-01

**DOI**
10.1074/jbc.m114.575621

Peer reviewed

# Hyaluronan Breakdown Contributes to Immune Defense against Group A *Streptococcus**

Nina N. Schommer[‡], Jun Muto[‡], Victor Nizet[§¶], and Richard L. Gallo[‡§1]

From the ‡Division of Dermatology, Department of Medicine, §Division of Pharmacology and Drug Discovery, Department of Pediatrics, and ¶Skaggs School of Pharmacy and Pharmaceutical Sciences, University of California, San Diego, La Jolla, California 92093

**Background:** The role of hyaluronan catabolism in group A *Streptococcus* (GAS) infection has not been studied.
**Results:** Hyaluronan size differentially influenced GAS infection *in vitro* and in mice.
**Conclusion:** Digestion of hyaluronan derived from either the bacterium or host enhances host immune defense.
**Significance:** Digestion of hyaluronan during GAS infection may be a previously unrecognized mechanism for host defense.

Group A *Streptococcus* (GAS) commonly infects human skin and occasionally causes severe and life-threatening invasive diseases. The hyaluronan (HA) capsule of GAS has been proposed to protect GAS from host defense by mimicking endogenous HA, a large and abundant glycosaminoglycan in the skin. However, HA is degraded during tissue injury, and the functions of short-chain HA that is generated during infection have not been studied. To examine the impact of the molecular mass of HA on GAS infection, we established infection models *in vitro* and *in vivo* in which the size of HA was defined by enzymatic digestion or custom synthesis. We discovered that conversion of high molecular mass HA to low molecular mass HA facilitated GAS phagocytosis by macrophages and limited the severity of infection in mice. In contrast, native high molecular mass HA significantly impaired internalization by macrophages and increased GAS survival in murine blood. Thus, our data demonstrate that GAS virulence can be influenced by the size of HA derived from both the bacterium and host and suggest that high molecular mass HA facilitates GAS deep tissue infections, whereas the generation of short-chain HA can be protective.

Skin and soft tissue infections occur frequently and range in severity from minor self-limiting superficial infections to life-threatening invasive diseases (1, 2). Uncomplicated superficial skin infections are often self-limited or can be managed effectively with topical or oral antibiotic treatment. However, deep tissue infections such as severe cellulitis and necrotizing fasciitis often evade host immune defense systems, are difficult to treat, and represent an important clinical challenge (3, 4).

*Streptococcus pyogenes* or group A *Streptococcus* (GAS)[2] is a major cause of skin and soft tissue infections. The pathogenesis of GAS skin and soft tissue infections is complex and multifactorial, involving numerous virulence factors that facilitate bacterial interactions with host tissues and evasion of the host's innate immune system (5). The host immune response to GAS remains incompletely defined. Initial defense mechanisms against GAS involve the chemical and physical barrier of the skin and skin microbiota. Antimicrobial peptides synthesized by epithelial cells and commensal bacteria represent important initial elements of cutaneous immunity against GAS (6, 7). However, disruption of the skin barrier can enable the bacterium to breach the epithelium and enter deeper dermal tissues. At this stage, bacteria encounter resident and recruited immune cells. GAS has been proposed to evade resident leukocyte killing by expressing on its surface a capsule consisting of long chains of hyaluronan (HA) to mimic the HA-rich surrounding environment of the dermis (5, 8).

HA is ubiquitously expressed in the extracellular matrix of all vertebrate tissues and is the most abundant glycosaminoglycan in the skin (9, 10). HA synthesis occurs at the plasma membrane, with the growing polymer being extruded into the extracellular environment, allowing the molecule to have a very large degree of polymerization and size ($>800$ kDa). In its native form, HA occupies a large hydrodynamic volume and has been assigned various physiological functions in the extracellular matrix, *e.g.* water homeostasis, structural organization, and protective lubricant for joint motion (11).

Despite its simple structure and ubiquitous distribution, HA is a dynamic molecule (12). Breakdown and turnover of HA occur both at steady state and upon injury. This breakdown is important because high molecular mass HA (HMM-HA) has distinct functions from low molecular mass HA (LMM-HA) (13–15). LMM-HA ($<75$ kDa) can be generated by hyaluronidase-mediated degradation or by tissue injury (16). Although native HA is reported to have anti-inflammatory functions, low molecular mass polymers signal tissue damage by stimulating a variety of immune cells at the injury site (17). Consequently, the distinct functions of HMM-HA and LMM-HA raise interesting questions about the role of HA mimicry in the course of GAS infection.

Herein, we hypothesized that the initial establishment of GAS skin infection is substantially influenced by the status and molecular mass of HA in the surrounding tissue. Our findings demonstrate that fragmentation of HMM-HA to LMM-HA

limits the capacity of GAS to resist phagocytosis and advance infection. Our results shed light on the complex and critical role of HA in infection and suggest that the breakdown of HA may provide an additional defense mechanism against this leading human skin pathogen.

## EXPERIMENTAL PROCEDURES

*Ethics Statement*—This study was carried out in strict accordance with the recommendations in the *Guide for the Care and Use of Laboratory Animals* of the National Institutes of Health. Experiments using mice were performed at University of California, San Diego, where the ethics committee specifically approved this study under Institutional Animal Care and Use Committee Protocol S09074.

*Animals*—Transgenic mice for conditional overexpression of human hyaluronidase-1 were generated as described previously (18) by combining a constitutive promoter and a loxP-flanked GFP reporter upstream of hyaluronidase-1 (CAG-loxP-GFPstop-loxP-Hya1). Cross-breeding with E2a-Cre mice for early embryonic expression of Cre enabled the promoter to drive the expression of the downstream hyaluronidase gene. WT and CD44$^{-/-}$ mice were obtained from The Jackson Laboratory.

*Bacteria*—GAS strain NZ131 is a well characterized T14/M49 glomerulonephritis isolate. Both NZ131 and the GAS capsule-deficient mutant 5448ΔhasA were obtained one of us (V. N.). GAS strains were propagated using Todd-Hewitt broth or 5% sheep blood agar (BD Biosciences). Erythromycin (5 μg/ml) for selection was used for the GAS mutant strain.

*Cell Culture*—The mouse alveolar cell line MH-S was purchased from American Type Culture Collection. Cells were cultured in RPMI 1640 medium supplemented with 2 mM L-glutamine, 10% heat-inactivated FBS, 100 units/ml penicillin, 50 μg/ml streptomycin, and an additional 50 μM 2-mercaptoethanol. For isolation of peritoneal macrophages, mice were injected intraperitoneally with 2 ml of 3% thioglycollate. After 72 h, primary macrophages were collected from euthanized animals by peritoneal lavage using 10 ml of sterile PBS. Cells were washed with RPMI 1640 medium with the supplements indicated above, plated onto 12-well tissue culture plates, and incubated at 5% $CO_2$ and 37 °C. Cells were washed daily and used for experimental procedures after 3 days.

*Cell Reagents*—HA polymers of specific sizes were obtained from Sigma-Aldrich (Select-HA Hyaluronan 50K, 25–75 kDa; and Select-HA Hyaluronan 1000K, 800–1200 kDa). Molarity was calculated with 25 and 800 kDa, respectively.

*In Vitro Infection Model*—Overnight cultures of GAS were diluted and incubated under static conditions to obtain GAS in exponential growth phase. While washing the bacteria with cold PBS, HA polymers at 20 μg/ml were added to macrophages adhering to glass coverslips in a 12-well plate format. The mixture of macrophages, HA fragments, and bacteria at a multiplicity of infection of 100 was spun down at 150 × g for 1 min. After the specific times indicated in each figure, infected samples were washed five times with ice-cold PBS and then prepared for immunofluorescence staining and microscopy by fixation with fresh 3.7% paraformaldehyde in PBS.

*Hyaluronidase Treatment in Vitro*—To test the effect of HA breakdown in macrophage infection with GAS *in vitro*, GAS or MH-S macrophages were pretreated with hyaluronidase for 1 h prior to infection. This hyaluronidase is derived from *Streptomyces hyalurolyticus* (Sigma-Aldrich). This enzyme was used at 9 units/ml in each experiment. As control, the enzyme was inactivated by boiling for 10 min.

*Whole Blood Killing Assay*—Fresh mouse blood was collected into 2-ml heparin blood collection tubes (BD Biosciences). HMM-HA or LMM-HA (20 μg) and 50 μl of 10% Todd-Hewitt broth in RPMI 1640 medium containing $1 \times 10^2$ cfu of freshly diluted log-phase GAS were added to 50 μl of blood/well in a 96-well format. The mixture was incubated for 4 h at 37 °C, followed by plating dilutions of the mixture on blood agar for enumeration of GAS cfu.

*Mouse Model of GAS Infection*—The susceptibility of WT and mutant mice to GAS infection was measured by modification of a previously described GAS infection model (6, 19). The backs of sex-matched adult mice were shaved, and hair was chemically removed with Nair hair remover lotion. Mice were injected subcutaneously with 100 μl of GAS NZ131 in PBS in exponential growth phase ($A_{600} = 0.5$; $2 \times 10^6$ cfu). Ulcer and whole lesion sizes were measured 24 and 48 h after GAS infection. Enumeration of cfu was performed by extraction of biopsies from infected animals, tissue homogenization, and overnight incubation on blood agar plates.

*Quantification of GAS inside or outside of Macrophage Cells by Differential Immunostaining*—Localization of GAS bacteria during infection of the macrophage cell line MH-S or primary macrophages was determined using the double-fluorescence immunostaining method described previously (20, 21). This method is based on the application of two different fixation methods. Infected macrophages were incubated with fresh 3.7% paraformaldehyde in PBS, which leaves the cell membrane impermeable. Thus, all bacteria outside of the cell and on the cell surface, respectively, were made visible using an anti-GAS antibody (Abcam) plus an Alexa Fluor 488 antibody (Invitrogen). Permeabilization of macrophages was achieved by the addition of Triton X-100, which allowed the staining of all internalized bacteria (plus all bacteria outside of the cell) with the same primary anti-GAS antibody but with a different secondary antibody (Alexa Fluor 568, Invitrogen). Coverslips mounted with ProLong Gold antifade reagent with DAPI (Invitrogen) were examined by conventional fluorescence microscopy (Olympus BX41).

*Determination of Phagocytosis*—To test whether GAS bacteria were phagocytized by macrophages, MH-S or peritoneal cells were incubated with 5 μg/ml cytochalasin B derived from *Drechslera dematioidea* (Sigma-Aldrich) prior to infection with GAS. Analysis was performed by double-fluorescence immunostaining as described above.

*Statistical Analysis*—Statistical analysis was performed using Prism version 5.0 software (GraphPad Software Inc., La Jolla, CA). The means ± S.E. were calculated for each data set. Data were analyzed by analysis of variance or the Kruskal-Wallis test with post-tests when appropriate, the Mann-Whitney *U* test, and the unpaired *t* test.
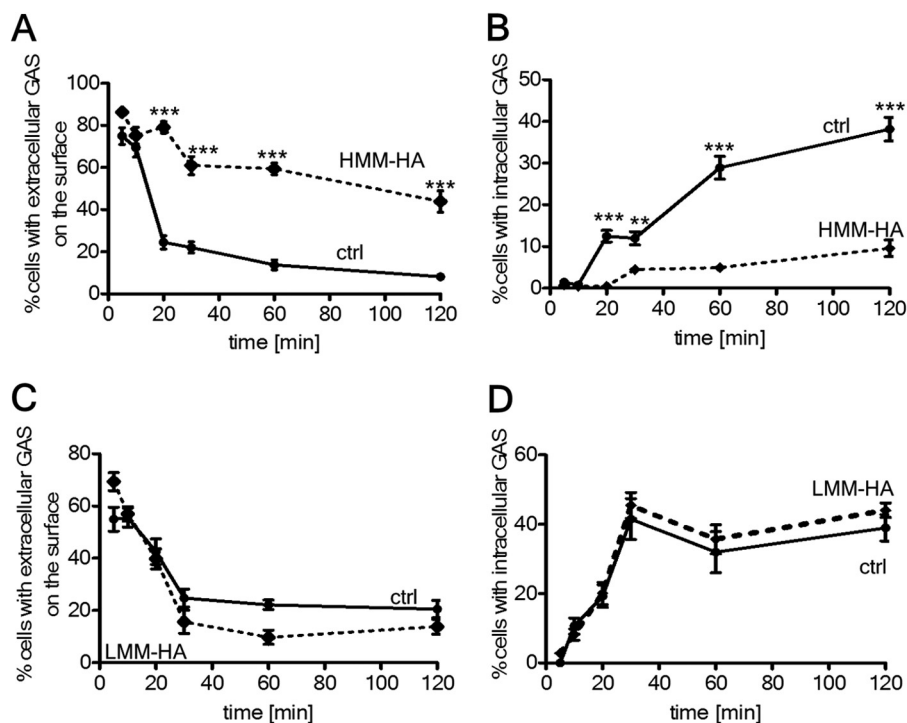
FIGURE 1. **The molecular mass of HA influences GAS internalization in macrophages.** MH-S macrophages were exposed to GAS and left untreated (control; *solid line*) or were treated with either HMM-HA (25 nM, 20 $\mu$g/ml) (*A* and *B*) or LMM-HA at the same molar concentration (25 nM, 0.625 $\mu$g/ml). After the indicated times of exposure, cells were fixed, MH-S nuclei were stained with DAPI, and extracellular bacteria were distinguished from intracellular bacteria by differential immunostaining. Enumeration of GAS associated with MH-S cells was done by assigning them as cells with mainly extracellular GAS on their surface (*A* and *C*) or as cells with mainly internalized GAS. HMM-HA increased the number of group A streptococci that failed to internalize (*A* and *B*), whereas LMM-HA slightly increased the uptake of GAS by MH-S cells (*C* and *D*). Data are shown as the percentage of cells with either extracellular or intracellular GAS and represent the mean ± S.E. of nine counts in each group (one count = all cells in one microscopic vision field). **, $p < 0.01$; ***, $p < 0.001$. Cells treated with HA are shown as *dashed lines*, and the controls (*ctrl*) are shown as *solid lines*.

## RESULTS

*HMM-HA Limits Phagocytosis of GAS*—To determine whether the size of HA influences phagocytosis of GAS by macrophages, we established an *in vitro* model in which either large HMM-HA (800–1200 kDa) or small LMM-HA (25–75 kDa) was added to the culture medium of MH-S murine macrophages in the presence of GAS. Uptake of bacteria was measured over time by differential immunostaining of GAS at the cell surface or within the cell. Quantification of this process confirmed that GAS remained largely at the cell surface in the presence of HMM-HA compared with control untreated cells (Fig. 1, *A* and *B*) or those treated with LMM-HA at a similar molar concentration (Fig. 1, *C* and *D*). Direct visualization showed a large effect on macrophage uptake of GAS in untreated cells (Fig. 2, *A* and *B*) compared with those treated with HMM-HA (Fig. 2, *C* and *D*) or an equal mass of LMM-HA (Fig. 2, *E* and *F*). These findings show that HA polymers of different size have different effects on GAS entry into macrophages and that HMM-HA, such as that found endogenously in normal skin, may trap GAS at the cell surface and inhibit uptake. To further extend these observations to a model primarily dependent on neutrophil killing, we evaluated GAS killing in whole blood in the presence of HA polymers. Consistent with the findings of inhibition of phagocytosis observed with MH-S cells, significantly higher GAS survival was observed when HMM-HA was added to the blood killing assay (Fig. 3).

*Hyaluronidase Enhances the Uptake of GAS by Macrophages*—Having observed that HMM-HA limits macrophage uptake of GAS, we next evaluated if the breakdown of HA that takes place during tissue injury (16) might have an opposing effect on the capacity of host macrophages to fight the pathogen. The addition of hyaluronidase to cell culture medium increased the number of group A streptococci internalized by macrophages (Fig. 4*A*); control experiments done with heat-inactivated hyaluronidase demonstrated no effect on uptake (Fig. 4*B*). Interestingly, when macrophages and bacteria were incubated separately with hyaluronidase for 1 h prior to infection, treatment of either bacteria or MH-S cells with hyaluronidase was sufficient to influence GAS uptake (Fig. 4*A*). This finding indicates that HA at both the macrophage surface and in the capsule of GAS influences this host-pathogen interaction.

*Macrophages Overexpressing Hyaluronidase-1 Show Increased Phagocytosis of GAS*—To more clearly understand the potential role of endogenous hyaluronidase action in the ability of macrophages to phagocytize GAS, we next evaluated peritoneal macrophages derived from transgenic mice conditionally overexpressing human hyaluronidase (*HYAL1*) (18). The expression of this gene has been previously shown to digest tissue HA to generate small HA fragments (~27 kDa) and results in depletion of HMM-HA from tissues (18). Paralleling results with the MH-S macrophage cell line, peritoneal macrophages from WT mice incubated with HMM-HA had increased GAS remaining at the cell surface and fewer intracellular group A streptococci
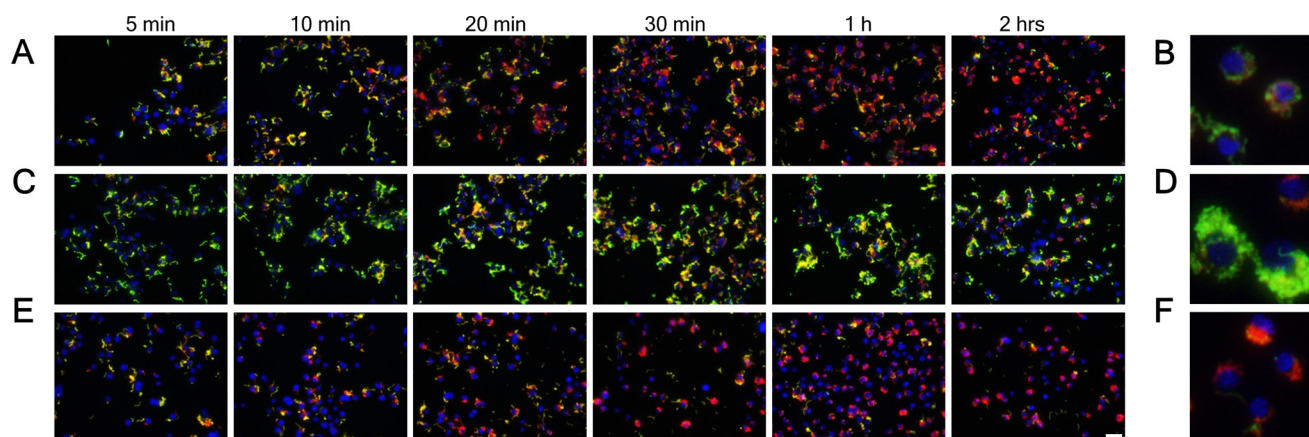
**FIGURE 2. Visualization of macrophages exposed to GAS in the presence of HA polymers.** MH-S macrophages were exposed to GAS at a multiplicity of infection of 100 and left untreated (*A* and *B*) or were treated with either HMM-HA (*C* and *D*) or LMM-HA (*E* and *F*) at a concentration of 20 $\mu$g/ml. After the indicated times of infection, MH-S cells and bacteria were stained as described in the legend to Fig. 1. *B*, *D*, and *F* represent image magnifications of three to four single cells. Extracellular bacteria are *green-yellow*, and intracellular bacteria are *red*. *Scale bar* = 20 $\mu$m.
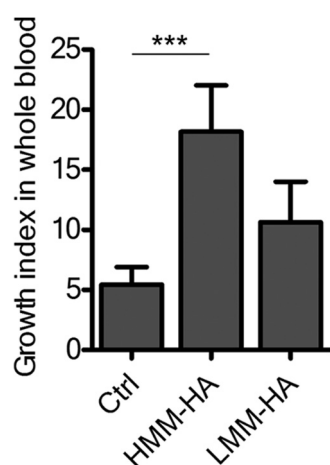


**FIGURE 3. HMM-HA induces increased survival of GAS in murine blood.** Shown is the GAS-killing activity of mouse whole blood either with no further treatment (control (*Ctrl*)) or with the addition of HMM-HA or LMM-HA (20 $\mu$g/ml). Data are expressed as the growth index (cfu of bacteria after 4 h of incubation in blood *versus* initial cfu of bacteria) and represent the mean $\pm$ S.E. of 12 replicates of two mice in each group. ***, $p < 0.002$.

compared with peritoneal macrophages incubated with LMM-HA (Fig. 4, *C* and *D*). However, peritoneal macrophages derived from transgenic mice overexpressing *HYAL1* exhibited a high level of GAS uptake even when HMM-HA was added. This effect mirrored the increase in intracellular GAS found upon the addition of LMM-HA to macrophages, suggesting that macrophage overexpression of hyaluronidase results in digestion of HMM-HA to convert its action to resemble that of LMM-HA. This change in function is consistent with prior observations on the capacity of these cells to digest HMM-HA to its LMM form (18).

*CD44 Influences the Effect of HA on Macrophage Uptake of GAS*—Binding of HA to the cell surface receptor CD44 is involved in diverse events, including attachment, organization, and turnover of the extracellular matrix at the cell surface, as well as the mediation of lymphocyte migration during inflammation (22). Peritoneal macrophages derived from CD44$^{-/-}$ mice had higher GAS concentrations at the cell surface under control conditions and after the addition of LMM-HA (Fig. 5*A*). This suggested that the baseline binding of GAS to macro-

phages was inhibited by CD44. Furthermore, no further increase in cell surface-associated GAS was seen when CD44$^{-/-}$ cells were exposed to HMM-HA (Fig. 5*A*). This observation suggested that the effects of HMM-HA were dependent on CD44. Supporting this, no effect on GAS internalization could be observed in CD44$^{-/-}$ macrophages when HMM-HA was added to the cell culture medium (Fig. 5*B*). Similar results were observed at short (30 min) incubation times of GAS and macrophages (Fig. 5, *C* and *D*). Visualization of GAS associated with macrophages derived from WT and CD44$^{-/-}$ mice confirmed that GAS was trapped primarily outside when CD44 was absent (Fig. 5, *E* and *F*). These observations show an important role for CD44 in mediating GAS uptake into macrophages and suggest that HMM-HA may act through CD44 to inhibit uptake.

*GAS Infection Is Decreased in Transgenic Mice Overexpressing Hyaluronidase-1*—Because HMM-HA limited GAS entry into macrophages and blood killing and because LMM-HA or hyaluronidase expression enhanced bacterial uptake, we next examined the influence of HA digestion on infection *in vivo*. Normal skin wounding is known to result in breakdown of HA to its LMM form and the activation of an inflammatory process (16). To determine the influence of hyaluronidase on GAS infection in the absence of prior stimulation of inflammation, it was necessary to examine a model of HA breakdown without prior skin injury. *HYAL1* expression in mice results in no spontaneous inflammation or histological evidence of injury but effectively reduces the size of dermal HA to a LMM form (18). Direct subcutaneous inoculation of GAS into these mice permitted analysis of the role of HA size *in vivo* without prior activation of immunity. Consistent with predictions from experiments done *in vitro*, *HYAL1*-overexpressing mice with a lack of HMM-HA were more resistant to GAS infection compared with WT mice (Fig. 6, *A–C*) and had decreased cfu recovered from the lesion (Fig. 6*D*).

*HA and CD44 Influence GAS Infection by Multiple Mechanisms*—As we demonstrated that CD44 binding is essential for mediating the effects of HA on macrophages *in vitro*, we next assessed if this cell surface receptor is important for the progression of subcutaneous infection *in vivo* using four groups of mice: 1)
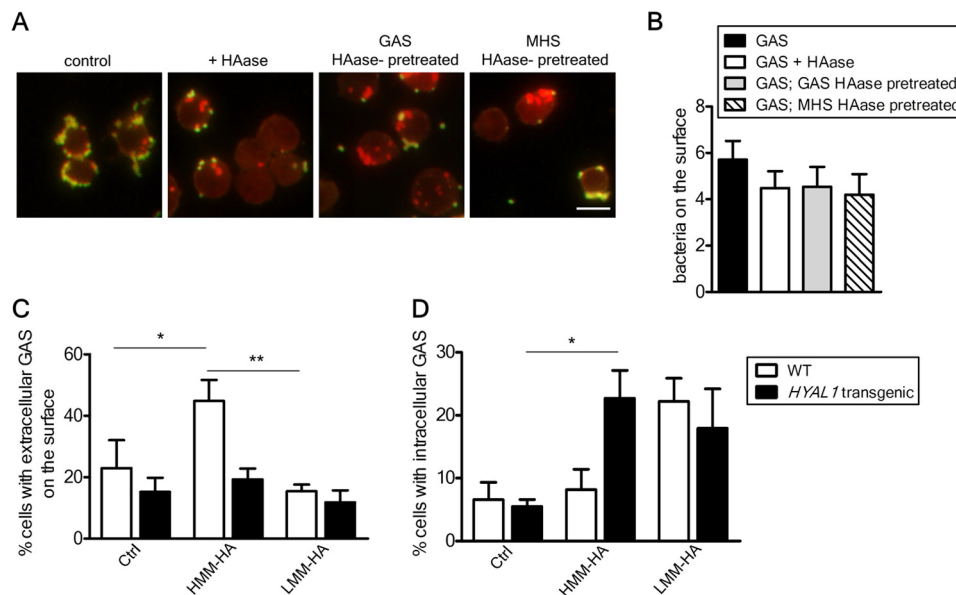
FIGURE 4. **Hyaluronidase inhibits the entrapment of GAS at the surface of macrophages and leads to increased internalization.** *A*, MH-S macrophages were exposed to GAS and either left untreated or incubated together with hyaluronidase (*HAase*) for 2 h. For comparison, MH-S cells were separately pretreated with hyaluronidase for 1 h and then exposed to GAS for 2 h, or GAS was pretreated with hyaluronidase for 1 h and then added to the macrophages for 2 h. Extracellular bacteria are *green-yellow*, and intracellular bacteria are *red*. *Scale bar* = 10 $\mu$m. *B*, inactivating hyaluronidase reversed entrapment of GAS on the cell surface. Hyaluronidase from *S. hyalurolyticus* was inactivated by boiling for 10 min prior to the experimental procedure as described for *A*. Enumeration of bacteria on the macrophage surface was done by differential immunostaining. After boiling, *S. hyalurolyticus* had no effect on GAS entrapment. *C* and *D*, overexpression of human hyaluronidase-1 in mouse peritoneal macrophages led to increased internalization of GAS and reversed the effects of HMM-HA. Peritoneal macrophages were extracted from WT mice (*white bars*) and *HYAL1*-overexpressing transgenic mice (*black bars*) and infected with GAS in the presence of either HMM-HA or LMM-HA. Control (*Ctrl*) samples were not incubated with HA. Similar to experiments with the MH-S cell line, HMM-HA diminished internalization of GAS by mouse peritoneal macrophages, whereas LMM-HA increased internalization. No increase in bacteria on the surface was seen when cells derived from *HYAL1*-overexpressing transgenic mice were treated with HMM-HA, but an increase in GAS internalization was seen in the presence of HMM-HA that was similar to LMM-HA. Values are the mean $\pm$ S.E. of nine counts in each group. *, $p < 0.03$; **, $p < 0.01$.

WT mice, 2) *HYAL1*-overexpressing mice, 3) mice deficient in CD44, and 4) *HYAL1*-overexpressing mice deficient in CD44. GAS infection was diminished when *HYAL1* was overexpressed in both the WT and CD44$^{-/-}$ background (Fig. 6, *E* and *F*). These observations suggest that the effect of *HYAL1* overexpression on infection was not limited to the effects upon macrophage entry seen in Fig. 5 because, in this mouse model, CD44 expression did not abolish the protective effect of *HYAL1* expression.

## DISCUSSION

In this study, we have demonstrated that the size of extracellular HA influences the capacity of macrophages to ingest GAS. Consistent with this observation, constitutive digestion of tissue HA limited the extent of GAS infection in mice. These observations show that GAS virulence is not only dependent on bacterial HA capsule expression, as presumed previously, but is also dictated and controlled by host HA. Our data therefore provide new insight into the complex interactions between the host and GAS and illustrate a previously unsuspected role for the extracellular matrix in this bacterial infection.

A hallmark of tissue injury is the turnover of extracellular matrix components (23). Fragmented HA accumulates during tissue injury and functions distinctly from the native polymer by serving as a danger-associated molecular pattern (17). Recognition of danger-associated molecular patterns is dependent on pattern recognition receptors such as the Toll-like receptors. Defense against invading pathogens is also dependent on Toll-like receptor recognition of the microbes themselves. We hypothesized that, under

physiological conditions, the response to infection will depend on both host HA and the microbe.

To test this hypothesis, we established GAS infection models *in vitro* and *in vivo* in which the size of HA was determined by custom synthesis or enzymatic digestion. The capacity of MH-S and primary macrophages to ingest GAS in the presence of LMM-HA was enhanced, suggesting increased activation of the macrophages. Surprisingly, HMM-HA modified the macrophage response by blocking phagocytosis and trapping bacteria on the cell surface. Interestingly, in prior studies of GAS infection, only the bacterial HA capsule has been suspected to play a major role in virulence (8, 24). Here, we have provided evidence that HA from both the host and bacterium will influence immune defense.

Our findings suggest that the digestion of HA observed during injury may be a host defense mechanism. We simulated this process by adding commercially available hyaluronidase (derived from *S. hyalurolyticus*) to the culture medium of macrophages in the presence of GAS. This enzyme hydrolyzes the hexosaminidic $\beta 1$–4 linkages between *N*-acetyl-D-glucosamine and D-glucuronic acid residues in HA, digesting the large polymer into fragments. Bacterial hyaluronidase treatment resulted in increased phagocytosis. Pretreating macrophages or GAS with hyaluronidase separately prior to infection resulted in similar observations. These data show that HA controls the phagocytosis of GAS in a manner dependent on its molecular mass, providing further evidence for a reciprocal relationship between host and bacterial HA.
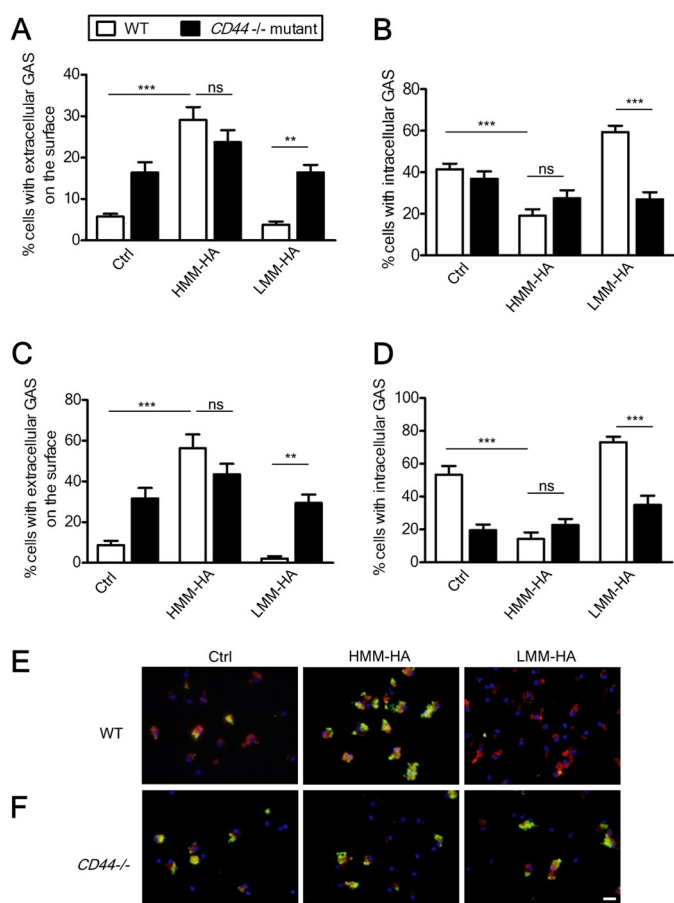
**FIGURE 5. Control of GAS internalization is dependent on CD44.** Peritoneal macrophages derived from CD44$^{-/-}$ and WT mice were exposed to GAS, and differential immunostaining was used to detect phagocytosis in macrophages with no further treatment (control (*Ctrl*)) or in the presence of HMM-HA or LMM-HA for 2 h. *White bars*, cells from WT control mice; *black bars*, cells from CD44$^{-/-}$ mice. *A*, percentage of peritoneal macrophages with predominant extracellular GAS. *B*, percentage of peritoneal macrophages with intracellular GAS. Peritoneal macrophages derived from CD44$^{-/-}$ mice showed increased extracellular bacteria but no significant differences when exposed to HMM-HA. *C* and *D*, similar results were obtained with 30 min of incubation for GAS and macrophages. Values represent the mean ± S.E. of two experiments with nine replicates/counts in each group (one count = all cells in one microscopic vision field). **, $p < 0.001$; ***, $p < 0.0001$; *ns*, not significant. *E* and *F*, GAS-infected peritoneal macrophages derived from either WT mice (*E*) or CD44$^{-/-}$ mice (*F*) in the presence of HA polymers by differential immunostaining and microscopy analysis. *Scale bar* = 20 μm.

**FIGURE 6. Transgenic mice overexpressing human hyaluronidase-1 have decreased GAS infection.** *A* and *B*, WT mice (*A*) and *HYAL1*-overexpressing transgenic mice (B) following subcutaneous inoculation with 2 × 10$^6$ cfu of GAS into back skin tissue. *Scale bars* are shown in centimeters. *C*, area of lesion in WT mice (▲) and *HYAL1*-overexpressing transgenic mice (■) after 48 h of infection. *D*, GAS bacteria cultured from tissue biopsies of WT and *HYAL1*-overexpressing transgenic mice. Values represent the mean ± S.E. of evaluations in a minimum of four animals and are representative of four experiments. *, $p < 0.04$. *E* and *F*, protection against GAS by HA breakdown is dependent on multiple mechanisms *in vivo*. WT mice (▲), *HYAL1*-overexpressing transgenic mice (■), CD44$^{-/-}$ mice (♦), and *HYAL1*/CD44$^{-/-}$ transgenic mice (◇) were subcutaneously infected with GAS in back skin tissue. Shown are lesion measurements (*E*) and GAS bacteria cultured from tissue biopsies after 48 h of infection (*F*). The greater infectious outcome of CD44 knock-out mice was shown to be diminished when *HYAL1* was overexpressed. *, $p < 0.002$.

To further test the influence of HA breakdown in GAS infection, we used a transgenic mouse model to conditionally overexpress human hyaluronidase *HYAL1* (18). These mice exhibit HA breakdown and generation of LMM-HA polymers of 27–500 kDa. Overexpression of human hyaluronidase in murine peritoneal macrophages reversed the entrapment of GAS on the macrophage surface caused by HMM-HA. Thus, GAS was internalized by the phagocytes once HMM-HA was digested. These results support observations from our *in vitro* experiments with hyaluronidase derived from *S. hyalurolyticus*.

The physiological relevance of HA breakdown in GAS infection was confirmed in our *in vivo* experiments. Transgenic mice overexpressing *HYAL1* had smaller lesions compared with WT mice, and biopsy and quantitative culture of the lesions from GAS-infected *HYAL1*-overexpressing transgenic mice showed significantly more microbial clearing compared with samples
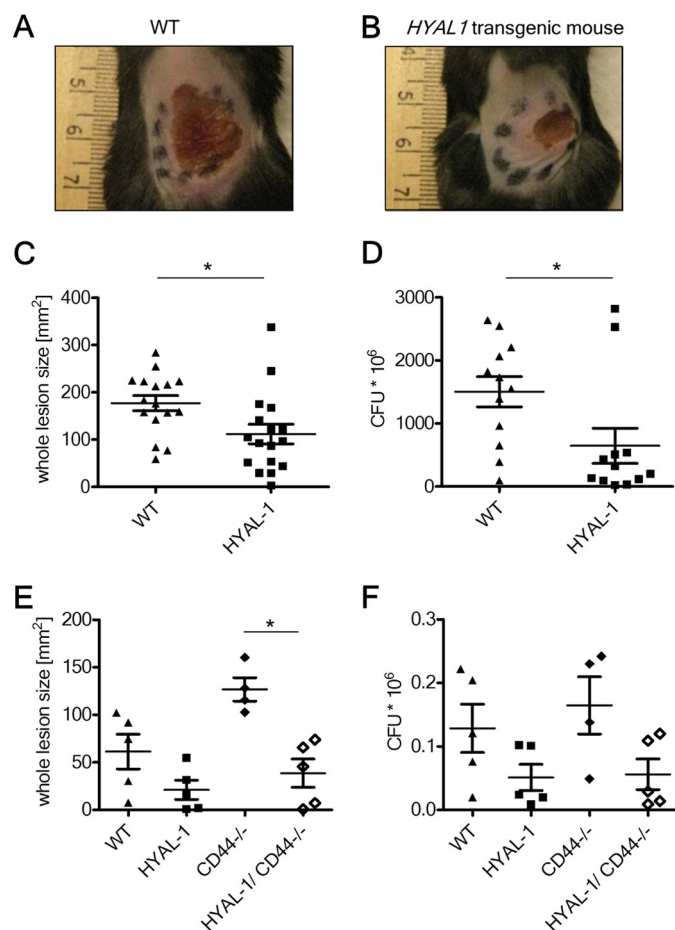
extracted from WT mice. Thus, in a model system in which invasion was bypassed by direct inoculation of bacteria, the action of hyaluronidase-1 in murine skin decreased GAS virulence.

^{13}C NMR studies have suggested that HMM-HA forms specific stable tertiary structures in aqueous solution, but this cooperative structure was not observed in LMM-HA solutions (25). The different structural propensities of HMM-HA and LMM-HA lead to the assumption that the molecular mass also influences the specific function of the molecule. It is conceivable that host- and bacterium-derived HMM-HA, unlike LMM-HA, does not interact with the appropriate receptor due to steric hindrance. In contrast, the differential structure of LMM-HA might allow the molecule to interact with the receptor and thereby induce a signaling cascade that eventually leads to phagocytosis of GAS by the macrophage.

Distinct functions of LMM-HA and HMM-HA have also been reported in other contexts (13–15, 26, 27). For instance, binding of LMM-HA to CD44 has been demonstrated to stimulate cell proliferation (26), whereas HMM-HA exerts an inhibitory effect (27). Based on these observations, HMM-HA and LMM-HA have different effects on CD44 clustering (15). As CD44 also contributes to the ingestion and clearance of particles (28) and has additional functions in inflammation and immune responses, we tested whether CD44 is involved in the underlying mechanism of HA-dependent control of infection. Peritoneal macrophages derived from CD44$^{-/-}$ mice showed no differences in GAS phagocytosis when exposed to HMM-HA or LMM-HA, suggesting that the underlying mechanism for control of phagocytosis by HA is related to CD44 and that CD44 is important for host defense. However, CD44 has also been reported to serve as a receptor for GAS adherence to keratinocytes (29) and pharyngeal epithelial cells (30) and may therefore participate in GAS virulence. Indeed, the GAS HA capsule impairs keratinocyte (29, 31) and macrophage (32) uptake of the pathogen and aids biofilm formation (31). In our comparison of CD44$^{-/-}$ and WT mice, we saw evidence for both functions. Although *HYAL1* expression could mitigate the worsened infectious outcome in the CD44-deficient phenotype in lesion size, quantitative cultures of the lesions from GAS-infected CD44$^{-/-}$ and *HYAL1*/CD44$^{-/-}$ mice yielded similar bacterial density/g of tissue. Thus, it is apparent that the control of GAS infection by CD44 is dependent on multiple mechanisms. Although CD44 is widely seen as a major cell surface receptor for HA, the molecule equally binds to other proteins to exert its functions (33). In this context, it cannot be excluded that another receptor of HA might also play an important role in the control of GAS infection by HA.

In conclusion, our data highlight HA as a critical factor for defense against GAS infection. Our findings extend the spectrum of activities of HA and shed light on why GAS is so resistant in deep tissue infections. The findings support a new hypothesis that bacteria may exploit large HA from the host extracellular matrix to avoid killing. The initial defense against GAS in wounds may be driven by the local digestion of HMM-HA and facilitated by production of LMM-HA. These observations could enable innovative approaches for the treatment of GAS disease.

## REFERENCES

1. Lin, J. N., Chang, L. L., Lai, C. H., Lin, H. H., and Chen, Y. H. (2011) Clinical and molecular characteristics of invasive and noninvasive skin and soft tissue infections caused by group A *Streptococcus. J. Clin. Microbiol.* **49,** 3632–3637
2. DiNubile, M. J., and Lipsky, B. A. (2004) Complicated infections of skin and skin structures: when the infection is more than skin deep. *J. Antimicrob. Chemother.* **53,** Suppl. 2, ii37–ii50
3. Nathwani, D. (2009) New antibiotics for the management of complicated skin and soft tissue infections: are they any better? *Int. J. Antimicrob. Agents* **34,** Suppl. 1, S24–S29
4. Giordano, P., Weber, K., Gesin, G., and Kubert, J. (2007) Skin and skin structure infections: treatment with newer generation fluoroquinolones. *Ther Clin. Risk Manag.* **3,** 309–317
5. Cole, J. N., Barnett, T. C., Nizet, V., and Walker, M. J. (2011) Molecular insight into invasive group A streptococcal disease. *Nat. Rev. Microbiol.* **9,** 724–736
6. Nizet, V., Ohtake, T., Lauth, X., Trowbridge, J., Rudisill, J., Dorschner, R. A., Pestonjamasp, V., Piraino, J., Huttner, K., and Gallo, R. L. (2001) Innate antimicrobial peptide protects the skin from invasive bacterial infection. *Nature* **414,** 454–457
7. Cogen, A. L., Yamasaki, K., Muto, J., Sanchez, K. M., Crotty Alexander, L., Tanios, J., Lai, Y., Kim, J. E., Nizet, V., and Gallo, R. L. (2010) Staphylococcus epidermidis antimicrobial δ-toxin (phenol-soluble modulin-γ) cooperates with host antimicrobial peptides to kill group A *Streptococcus. PLoS ONE* **5,** e8557
8. Wessels, M. R., Moses, A. E., Goldberg, J. B., and DiCesare, T. J. (1991) Hyaluronic acid capsule is a virulence factor for mucoid group A streptococci. *Proc. Natl. Acad. Sci. U.S.A.* **88,** 8317–8321
9. Tammi, R., Ripellino, J. A., Margolis, R. U., and Tammi, M. (1988) Localization of epidermal hyaluronic acid using the hyaluronate binding region of cartilage proteoglycan as a specific probe. *J. Invest. Dermatol.* **90,** 412–414
10. Dicker, K. T., Gurski, L. A., Pradhan-Bhatt, S., Witt, R. L., Farach-Carson, M. C., and Jia, X. (2014) Hyaluronan: a simple polysaccharide with diverse biological functions. *Acta Biomater.* **10,** 1558–1570
11. Tammi, M. I., Day, A. J., and Turley, E. A. (2002) Hyaluronan and homeostasis: a balancing act. *J. Biol. Chem.* **277,** 4581–4584
12. Laurent, T. C., and Fraser, J. R. (1992) Hyaluronan. *FASEB J.* **6,** 2397–2404
13. Tian, X., Azpurua, J., Hine, C., Vaidya, A., Myakishev-Rempel, M., Ablaeva, J., Mao, Z., Nevo, E., Gorbunova, V., and Seluanov, A. (2013) High-molecular-mass hyaluronan mediates the cancer resistance of the naked mole rat. *Nature* **499,** 346–349
14. Hill, D. R., Rho, H. K., Kessler, S. P., Amin, R., Homer, C. R., McDonald, C., Cowman, M. K., and de la Motte, C. A. (2013) Human milk hyaluronan enhances innate defense of the intestinal epithelium. *J. Biol. Chem.* **288,** 29090–29104
15. Yang, C., Cao, M., Liu, H., He, Y., Xu, J., Du, Y., Liu, Y., Wang, W., Cui, L., Hu, J., and Gao, F. (2012) The high and low molecular weight forms of hyaluronan have distinct effects on CD44 clustering. *J. Biol. Chem.* **287,** 43094–43107
16. Taylor, K. R., Yamasaki, K., Radek, K. A., Di Nardo, A., Goodarzi, H., Golenbock, D., Beutler, B., and Gallo, R. L. (2007) Recognition of hyaluronan released in sterile injury involves a unique receptor complex dependent on Toll-like receptor 4, CD44, and MD-2. *J. Biol. Chem.* **282,** 18265–18275
17. Scheibner, K. A., Lutz, M. A., Boodoo, S., Fenton, M. J., Powell, J. D., and Horton, M. R. (2006) Hyaluronan fragments act as an endogenous danger signal by engaging TLR2. *J. Immunol.* **177,** 1272–1281
18. Muto, J., Morioka, Y., Yamasaki, K., Kim, M., Garcia, A., Carlin, A. F., Varki, A., and Gallo, R. L. (2014) Hyaluronan digestion controls DC migration from the skin. *J. Clin. Invest.* **124,** 1309–1319
19. Betschel, S. D., Borgia, S. M., Barg, N. L., Low, D. E., and De Azavedo, J. C. (1998) Reduced virulence of group A streptococcal Tn916 mutants that do not produce streptolysin S. *Infect. Immun.* **66,** 1671–1679
20. Schommer, N. N., Christner, M., Hentschke, M., Ruckdeschel, K., Aepfelbacher, M., and Rohde, H. (2011) Staphylococcus epidermidis uses distinct mechanisms of biofilm formation to interfere with phagocytosis and activation of mouse macrophage-like cells 774A.1. *Infect. Immun* **79,** 2267–2276
21. Heesemann, J., and Laufs, R. (1985) Double immunofluorescence microscopic technique for accurate differentiation of extracellularly and intracellularly located bacteria in cell culture. *J. Clin. Microbiol.* **22,** 168–175
22. Jiang, D., Liang, J., and Noble, P. W. (2007) Hyaluronan in tissue injury and repair. *Annu. Rev. Cell Dev. Biol.* **23,** 435–461
23. Midwood, K. S., Williams, L. V., and Schwarzbauer, J. E. (2004) Tissue repair and the dynamics of the extracellular matrix. *Int. J. Biochem. Cell Biol.* **36,** 1031–1037
24. Cunningham, M. W. (2000) Pathogenesis of group A streptococcal infections. *Clin. Microbiol. Rev.* **13,** 470–511
25. Scott, J. E., and Heatley, F. (1999) Hyaluronan forms specific stable tertiary structures in aqueous solution: a $^{13}$C NMR study. *Proc. Natl. Acad. Sci. U.S.A.* **96,** 4850–4855
26. Slevin, M., Krupinski, J., Gaffney, J., Matou, S., West, D., Delisser, H., Savani, R. C., and Kumar, S. (2007) Hyaluronan-mediated angiogenesis in

vascular disease: uncovering RHAMM and CD44 receptor signaling pathways. *Matrix Biol.* **26,** 58–68

27. Kothapalli, D., Flowers, J., Xu, T., Puré, E., and Assoian, R. K. (2008) Differential activation of ERK and Rac mediates the proliferative and antiproliferative effects of hyaluronan and CD44. *J. Biol. Chem.* **283,** 31823–31829

28. Vachon, E., Martin, R., Plumb, J., Kwok, V., Vandivier, R. W., Glogauer, M., Kapus, A., Wang, X., Chow, C. W., Grinstein, S., and Downey, G. P. (2006) CD44 is a phagocytic receptor. *Blood* **107,** 4149–4158

29. Schrager, H. M., Albertí, S., Cywes, C., Dougherty, G. J., and Wessels, M. R. (1998) Hyaluronic acid capsule modulates M protein-mediated adherence and acts as a ligand for attachment of group A *Streptococcus* to CD44 on

human keratinocytes. *J. Clin. Invest.* **101,** 1708–1716

30. Cywes, C., and Wessels, M. R. (2001) Group A *Streptococcus* tissue invasion by CD44-mediated cell signalling. *Nature* **414,** 648–652

31. Hollands, A., Pence, M. A., Timmer, A. M., Osvath, S. R., Turnbull, L., Whitchurch, C. B., Walker, M. J., and Nizet, V. (2010) Genetic switch to hypervirulence reduces colonization phenotypes of the globally disseminated group A *Streptococcus* M1T1 clone. *J. Infect. Dis.* **202,** 11–19

32. Whitnack, E., Bisno, A. L., and Beachey, E. H. (1981) Hyaluronate capsule prevents attachment of group A streptococci to mouse peritoneal macrophages. *Infect. Immun.* **31,** 985–991

33. Jackson, D. G. (2009) Immunological functions of hyaluronan and its receptors in the lymphatics. *Immunol. Rev.* **230,** 216–231